Acta Astronautica 189 (2021) 391–397

Contents lists available at ScienceDirect

Acta Astronautica

journal homepage: www.elsevier.com/locate/actaastro

Research paper

Laboratory experiments with a laser-based attachment mechanism for spacecraft at small bodies

Niklas Anthony [a,*], Jan Frostevarg [b], Heikki Suhonen [c], Mikael Granvik [a,c]

[a] Asteroid Engineering Lab, Space Systems, Luleå, University of Technology, Box 848, 98128 Kiruna, Sweden
[b] Department of Engineering Sciences and Mathematics, Luleå, University of Technology, E-Huset, 97754 Luleå, Sweden
[c] Department of Physics, University of Helsinki, P.O. Box 64, 00014, Finland

ARTICLE INFO

Keywords:
Spacecraft anchoring
Laser drilling
High-speed imaging
X-ray micro-tomography
Asteroid mining

ABSTRACT

We present the results of two sets of experiments that investigate laser-based metal-to-rock attachment techniques. Asteroids and comets have low surface gravity which pose a challenge to landers with moving parts. Such parts can generate torques and forces which may tip the lander over or launch it into deep space. Thus, if a lander on a small body is to have moving parts, the spacecraft must be equipped with an anchoring mechanism. To this end, we sought to use a laser to melt and bind a piece of metal mimicking a part of a spacecraft to a rock mimicking the surface of a typical asteroid. In the first set of experiments, extra material was not fed in during the processing. The second set were performed using a standard wire feeder used in laser welding, which added metal to the experiment during processing. During the first experiments, we discovered that a traditional weld, where two melt pools mix and solidify to form a strong bond, was not possible—the melt pools would not mix, and when they did, the resulting weld was extremely brittle. The second set of experiments resulted in a physico-mechanical bond, where a hole was drilled with a laser, and a wire was melted and fed into the hole. These latter experiments were successful in forming bonds as strong as 115 N. Such an attachment mechanism can also be used to maneuver small boulders on asteroid surfaces, to redirect small, monolithic asteroids, or in space-debris removal.

1. Introduction

Landing (and staying anchored) on a small body such as an asteroid or comet is a challenge due to the micro-gravity environment. The surface gravity of a 1-km-diameter asteroid (assuming a spherical shape and uniform density of $3000\,\mathrm{kg/m^3}$) is 0.004% of Earth's gravity. The corresponding escape velocity is only $65\,\mathrm{cm/s}$, meaning if a spacecraft is launched or bounces off the surface at a higher speed, it will leave the gravity well of the asteroid entirely, and drift off into deep space. The 100-kg Philae lander, part of ESA's Rosetta mission, sought to tackle this challenge with a diverse suite of landing equipment: harpoons, thrusters, and screws. The thruster and harpoon failed to fire and the screws proved insufficient to hold the spacecraft down on their own, leading to a multiple-contact landing [1]. JAXA's Hayabusa2 mission had an alternative approach: three landers (1–10 kg in mass) were deployed from the main spacecraft, which had no landing gear at all, and were, instead, *designed* to bounce along the surface of asteroid (162173) Ryugu and these proved successful [2]. A summary of other anchoring techniques currently existing or in development is given in Zacny et al. 2013 [3].

We seek to understand the applicability of attaching metallic objects to natural materials using a laser. A potential scenario would play out as follows: a spacecraft approaches and hovers above the surface of an asteroid, lowers an anchoring unit that delivers a laser (via fiber-optic cable) and a wire feeder down to the surface, and welds the wire to a rock with the laser. The spacecraft can then be winched down with the same mechanism that lowered the anchoring unit. If the wire unintentionally breaks, more can be fed to the surface and reattached. The wire can also be intentionally cut with the laser to allow the spacecraft to move to a new location. This anchoring technique could also be used to redirect small asteroids or even space debris: rather than using the anchored wire as a winch point, the spacecraft can instead use its thrusters to pull on the object remotely (either for detumbling or for redirection). It can also be used for picking up monolithic rocks or boulders from the surface of an asteroid. This technique also has applications in space debris mitigation and removal.

Laser welding of two different materials is not a straightforward process. The differences in thermal, chemical, and physical properties lead to problems in controlling the quality of the weld joint. A review

* Corresponding author.
E-mail addresses: niklas.anthony@ltu.se, nik.sven@pm.me (N. Anthony).

https://doi.org/10.1016/j.actaastro.2021.08.028
Received 17 March 2021; Received in revised form 7 August 2021; Accepted 18 August 2021
Available online 28 August 2021

Table 1
Laser parameters.

Parameter	Value
Wavelength	1070 nm
Source power	<5000 W
Spot width	1 mm
Beam quality	8 mm mrad
Focal length	250 mm

of the methods for and challenges in welding aluminum and steel are described by Wang et al. 2016 [4]. Aluminum has a melting temperature between 800 K and 1000 K, where steel's is between 1600 K and 1700 K. Under the same laser irradiation, the aluminum will melt well before the steel, creating a lop-sided melt pool, which could be a source of pores and fractures. The melting point of olivine (one of the most abundant minerals thought to exist on asteroids) is between 1700 K and 2400 K, so attempting to join aluminum or steel to olivine will be a challenge. High-speed imaging (HSI) of laser processing of olivine shows a considerable amount of vapor bubbles during and after irradiation, and microscope images confirm that the re-solidified material has visible pores [5]. Other natural materials like pyroxene and serpentine (two other minerals common on asteroids) show similar behavior, and the re-solidified material is glassy.

2. Methodology

This research spans two sets of experiments, the first set did not achieve the intended outcome, but did provide critical information in forming the second set. In both cases, we assume that a spacecraft is capable of navigating to the surface of an asteroid, and either hover above the surface, or use alternative landing mechanisms to get to the surface. As the welding process takes less than 3 s, asteroid rotational effects are assumed negligible.

The first experiment was developed under the assumption that a piece of wire or landing leg was already resting on the surface of an asteroid, and a laser would sweep across it, melting part of the wire. The idea was that the re-solidified metal would bind to the surface like solder in a circuit board, with the wire still attached to the re-solidified mass. The spacecraft would then be able to apply tension to the wire, maintaining an anchoring force. To simulate this, a one-dimensional moving platform (CNC machine) was used to move the sample and the metal in tandem, keeping the processing laser and observation setup stationary. These experiments will be referred to in this paper as the moving-platform experiments (MPEs).

The second set of experiments were performed in a way that no material was already on the surface and the laser would remain stationary. A wire feeder (such as that used in typical welding processes) would feed wire into the laser beam, which would melt and form a soldered anchor. We hypothesized that using the laser to drill a hole before feeding the wire would allow more metal to form an anchor that extended below the surface. These experiments will be referred to as feeding experiments (FEs).

2.1. Methodology for moving-platform experiments

The first set of experiments were conducted with a YLS-5000 Ytterbium fiber laser from IPG Photonics, with the characteristics given in Table 1. The laser head was mounted 10° from vertical to prevent reflected processing light and ablated material from damaging the optics. Argon was pumped at 25 l/min to prevent oxidation of the metal and mineral. The minimum spot size allowed for a maximum power density of 637 kW/cm^2. For an experiment, the mineral (olivine) was clamped into a vice, and a metallic (312 R stainless steel) wire or plate was laid on the surface, taped on each end.

The HSI system used in this experiment is based on the one used by [6]. A high-speed camera (FASTCAM Mini UX100 type 800-M-16G) was configured to run at 10 000 frames per second (fps), with a 10 µs shutter speed. A narrow-pass filter allowing only 810 nm light through was placed in front of the lens of the camera and used in conjunction with an illumination laser of the same wavelength (CaviLux HF). This approach provided a clear view of the processing, which was captured at an angle roughly 25° above horizontal. An overview of the entire experiment setup is given in Fig. 1.

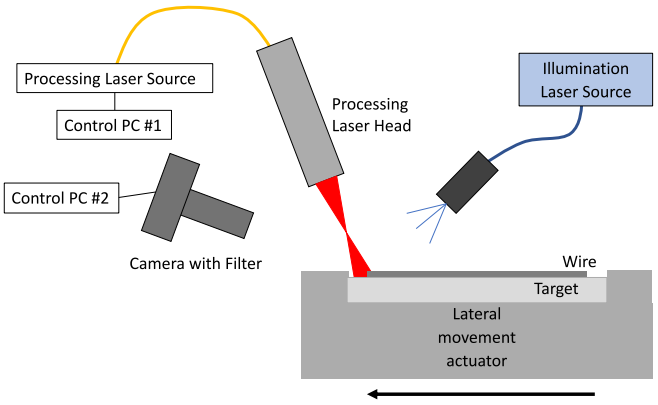

Fig. 1. Experiment setup. Not to scale.

Table 2
Laser parameters.

Parameter	Value
Wavelength	1070 nm
Source power	<15 000 W
Spot width	600 µm
Beam quality	10.5 mm mrad
Focal length	250 mm

The processing laser parameters were set using the software provided by IPG Photonics and the illumination laser was manually turned on and off as needed. The HSI laptop, running Photron FASTCAM Viewer software, was manually activated to acquire a 1.8-s video. A CNC script was configured to turn on the shielding gas and air crossjet (to protect the optics), activate the processing laser, move the sample, deactivate the laser, and then deactivate the gasses.

For a majority of the experiments, the laser power was ramped between two power levels along a fixed track length (between 3 cm and 5 cm), to see which power setting would produce the best weld seam. The laser on-time was calculated by dividing the length of a track by the movement rate of the sample (1 m/min).

2.2. Methodology for feeding experiments

The second set of experiments were performed with a YLR-15000-MM-WC Ytterbium fiber laser from IPG Photonics, with the characteristics given in Table 2. The HSI setup was configured to be the same as the first set of experiments, but the settings were different: 4000, frame size 1280 × 1024, 10 µs shutter time, total duration of 2.2 s. For longer experiments, the frame size was reduced to 1280 × 720 to increase the total duration of the exposure to 3.1 s. The observation angle was increased to roughly 45° from horizontal.

The laser head was mounted to a robotic arm at an angle 10° from vertical, again to prevent reflected processing light from damaging the optics. The spot size was set to 600 µm, allowing for power densities between up to 1760 kW/cm^2. Mison18 (18% CO_2, 82% Ar) was pumped at 25 l/min as a shielding gas to prevent oxidation. A 1.2-mm diameter stainless steel (R 312) wire spool was loaded into a TPS4000 VMT Remote feeder, with a Fronius GMA power source and configured to feed at a rate of 2.8 m/min, or 46.7 mm/s. The feeder head angle was configured to be as high as possible given the experiment geometry to

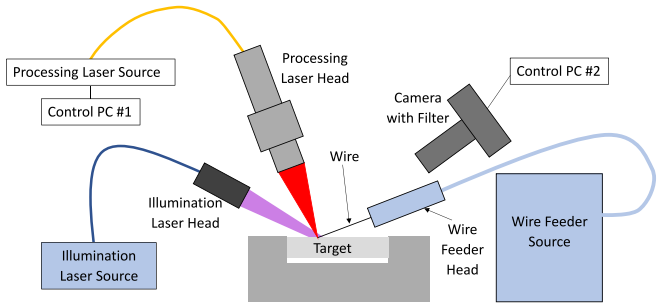

Fig. 2. Experiment setup.

simulate a spacecraft lowering the wire from "above" the surface. An illustration of the setup is shown in Fig. 2.

The processing laser parameters were set on a laptop using the software provided by IPG Photonics. The laser was configured to turn on upon receiving a signal from the robot arm. The laser would be on for a short time (~150 ms) to create a hole in the mineral. After the robot arm finished feeding the wire, it sent a second signal to turn off the laser. For some experiments, the power would be ramped down slowly while the wire continued to feed, or the feeding would continue for some time after the laser was turned off.

The robot arm's software also controlled the laser, gasses, and wire feeding. First, the argon gas was switched on, followed by the protective crossjet air gas. The arm would send a signal to the laser to begin processing, and after a fixed delay, would begin feeding wire into the experiment zone. After another fixed time, the arm sent a signal to the laser, which would either immediately turn off, or ramp down over a fixed time set in the laser software. After another fixed amount of time, the wire feeding would stop, and the gasses would be switched off.

The wire was then manually cut from the feeder head, and the sample moved to expose a fresh experiment site. As will be seen in the Results section, sometimes the anchored wires from previous experiments will be visible in the foreground or background of a given experiment.

2.3. Methodology for XMT analysis

The XMT measurements were carried out with a GE phoenix nanotom s system. The generator settings were 120 kV and 125 μA, and a 1-mm Cu filter was added to the beam. A total number of 1400 projection images with a pixel size of 33 μm were recorded over a 360° rotation with an exposure time of 2 × 250 ms for each image. The 3D volume data was reconstructed from these data sets using datos|x reconstruction software version 2.4.0.1199 (GE phoenix).

2.4. Methodology for anchor strength measurements

The strength of the attachment was tested using a Tinius Olsen H5KT Benchtop Tester using a 2.5-kN load cell. A custom sample holder was 3D printed using a ORIGINAL PRUSA I3 MK3S, to ensure the pull force was co-linear with the wire angle, see Fig. 3. The design includes selector pins inserted below and to the side of the sample, to align the desired pin with the direction of force.

Attaching the tester's upper (moving) arm to a wire proved difficult, but not impossible. Several attachment methods were tried, but the one successful one was to use two needle-nose pliers to bend the tip of the wire into a hook, which allowed a secure attachment point enough to perform the experiments. There was a concern that in the process of bending the wire, the anchor strength was weakened, so after the first two experiments (with the bent hook) the attachment mechanism was changed to an electrical conduit usually used to connect two loose wires.

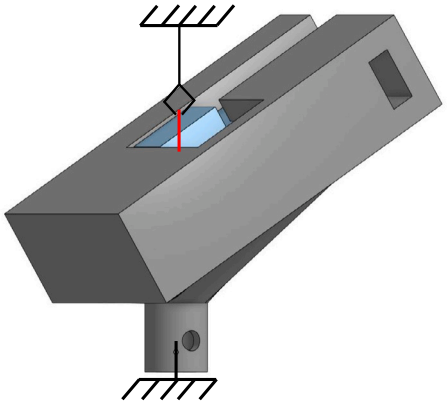

Fig. 3. Rendering of sample holder.

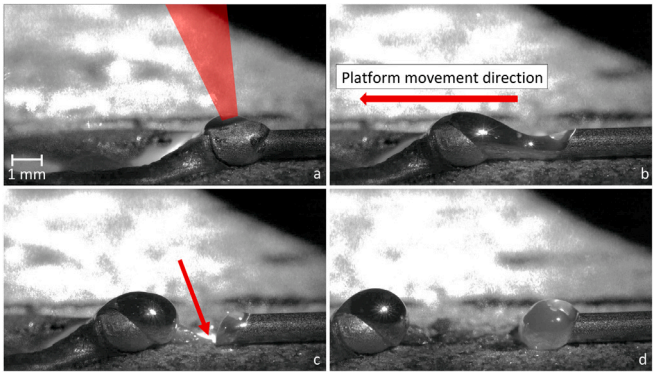

Fig. 4. High-speed footage of an attempt to weld a stainless steel wire to olivine. Seen in frame **a** is a crater caused by the delay between turning on the laser and moving the platform. It completely melted the wire, which formed a bulb on the right side of the frame, which was taken just as the laser spot began moving from the crater. Frame **b** is 288 ms later, after the laser has passed over the bulb, and began heating the wire, which are both molten. Just before frame **c** (at 308 ms), the wire breaks as a result of the surface tension from the bulb on the left and the molten bead on the right pulling it apart. The arrow shows that the laser spot is spanning both the wire and the olivine beneath. The final frame (**d** at 528 ms) shows the molten bead following the laser spot.

3. Results

3.1. Moving-platform experiments

The moving-platform experiments did not provide any result that had a solid attachment. The high-speed footage from these experiments showed two phenomena: the first being a lack of wetting, and the second being a lack of mixing of melt pools. The lack of wetting can be seen in Fig. 4d. As the platform moved, the laser would melt more of the wire, causing the molten bead to increase in size. The bead would remain cohesive, no matter the size, and glide across the sample's surface.

We hypothesized that above-mentioned phenomenon could have been due to the fact that the molten metal was allowed to *move* across the surface, so the wire was replaced with a sheet of metal. This experiment geometry would simulate the welding of a landing leg of a spacecraft that already landed on the surface of an asteroid. During the experiments with the sheets no moving metal bead formed. This too, however, did not achieve the intended result, as the two melt pools would not mix. This was exemplified by two further phenomena. First, a solid barrier would form between the two melt pools (Fig. 5). Second, any time the melt pools did come in direct contact, droplets of olivine would float to the top of the steel (Fig. 6) due to the difference in densities. Olivines can have densities in the range 3.2–4.4 g/cm^3 and steels can have densities in the range 7.85–8.67 g/cm^3.

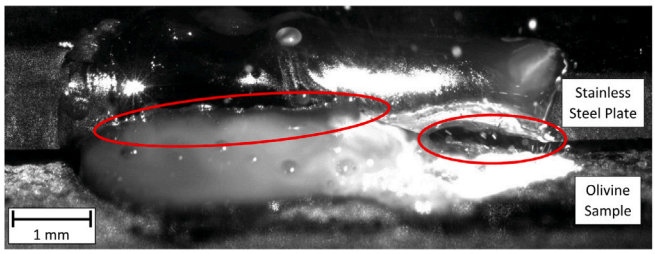

Fig. 5. High-speed footage of attempt to weld a stainless steel plate to olivine. The oval to the left shows a solid barrier between the two melt pools. The oval to the right shows a gap between the melt pools, probably due to sheet deformation and melt pool dynamics.

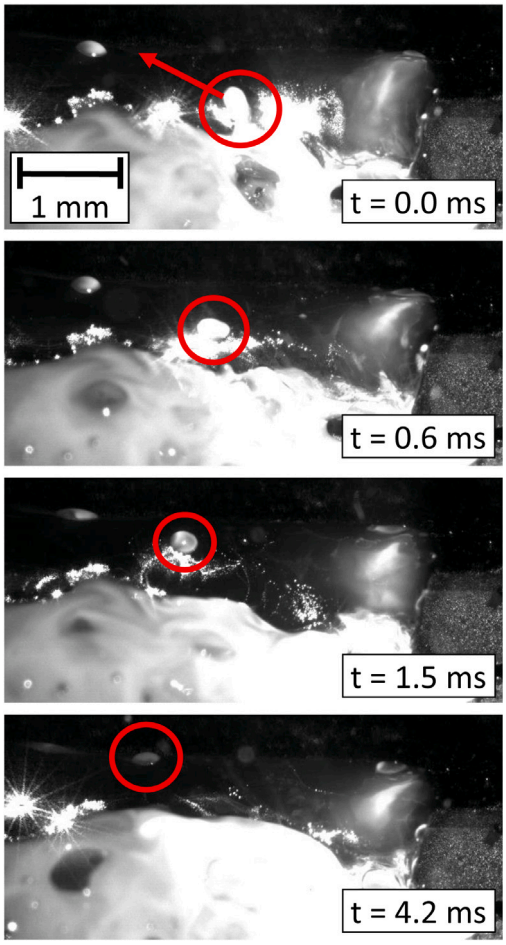

Fig. 6. Close-up of HSI from Fig. 5 showing a small droplet of molten olivine floating on top of the molten steel.

3.2. Feeding experiments

What became clear was that it was practically impossible to create a weld in the traditional sense, that is, a mixed melt pool that re-solidifies with the same (or similar) strength as the base materials. We decided to try a mechanical approach, where a hole would be drilled, and wire would be fed into it and melted. The molten metal would fill irregular shape of the hole, and the anchor force would be generated by friction, rather than a re-solidified mass. This would not require any new equipment for the spacecraft, it would simply be used in a different manner.

We began by estimating the size of a hole based on previous research [5], and calculating how long the feed time should be to fill

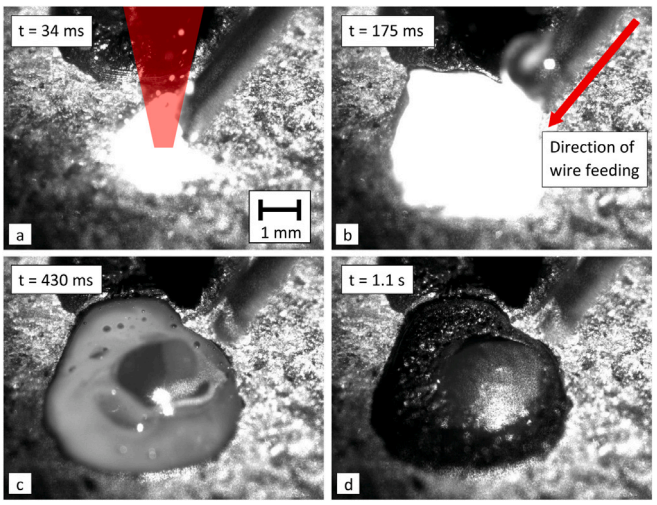

Fig. 7. High-speed footage of an experiment where the wire feed was stopped simultaneously with the laser. Frame **a** shows both the wire and olivine being processed moments after the laser was turned on. Frame **b** is roughly 50 ms after the wire began to be fed. Frame **c** shows the disconnect roughly 100 ms after the laser and wire feed stop. Frame **d** shows the result after cooling. In this experiment, the laser was turned on for 125 ms followed by another 125 ms, when both the laser and the wire feeder were operating, after which both were shut off simultaneously.

the hole with some excess on top. We aimed for a 10-mm-deep hole, so with a spot size of 0.6 mm, the volume was 2.82 mm^3, assuming a perfect cylinder. We set the laser power to 1500 W and used a volume removal efficiency of 15 mm^3/kJ. To make a hole this large, the laser would have to be on for 125 ms. To then fill the hole, the same volume of steel wire would need to be fed, in this case for 53 ms. We wanted a bit of material on top, so we elected to keep the feeder going for a total of 125 ms. We switched off the laser and wire feeder simultaneously, which had the effect of the molten metal on the sample surface to detach from the solid wire (see Fig. 7c). We note that due to delays in signal propagation, the timings were affected by a delay of roughly 10 ms, or 4% of the total time of the first experiment (250 ms).

We also expected a larger melt pool to form on the surface. For the next experiment, we increased the time that the feeder and laser were on to 500 ms, and allowed the feeder to continue feeding for an additional 500 ms after the laser was turned off. This resulted in what looks like a successful attachment (Fig. 8). An interesting phenomenon that occurred on this and subsequent experiments was an after-effect seen in Fig. 8f, where what appears to be re-solidified metal billows upwards, as if a bubble is being pushed up from below the surface.

In total, seven anchors were strong enough to be removed from the experiment platform whereas the other eight either fell off as the wire was cut from the wire feeder or from moving the sample from the stand (Fig. 9).

3.2.1. XMT analysis

An XMT scan revealed that varying the laser parameters does have an effect on the depth of penetration of the wire (Fig. 10). It appears that for each experiment, there is about 1–2 mm of re-solidified molten material above the surface and 1–2 mm below the surface, both forming a plug that sits at the entrance of the hole. Depths range from roughly 1 mm (#5) up to 9 mm (#6), and each one appears bent below the surface, following the shape of the hole as it was fed in. The given angle (58°) is from horizontal and represents the angle at which the wire was fed into the system for each experiment.

A detailed view of the holes produced by the laser shows a considerable amount of air surrounding the wires in the holes (Fig. 11). It also shows that the wire appears to be mostly intact below the surface, albeit slightly bent. There are also some bulges and bumps along the

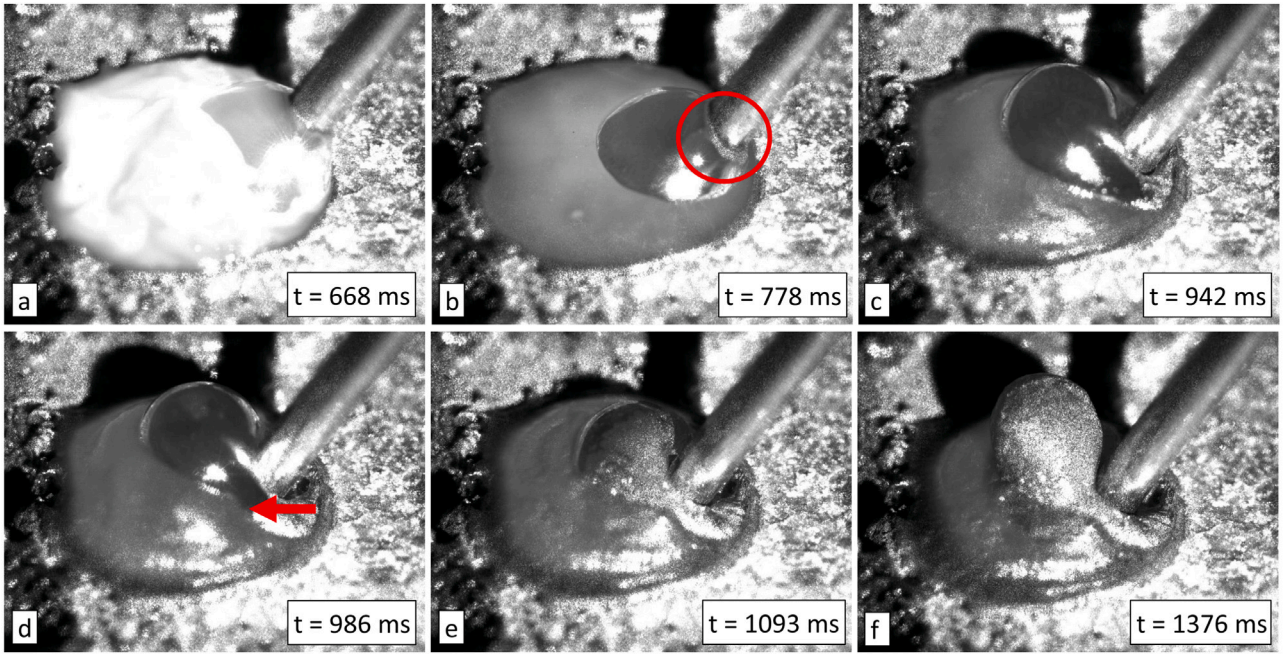

Fig. 8. High-speed footage of experiment where the wire feeding was allowed to continue for an additional 500 ms after the laser was turned off. At 668 ms, frame **a**, the laser is just being turned off. The molten metal begins to solidify starting close to the relatively cold solid wire, see the circle in frame **b**. This continues to the point that the wire physically shifts to the left before settling down (the red arrow in frame **d**)). The billowing phenomenon is seen in frame **f**).

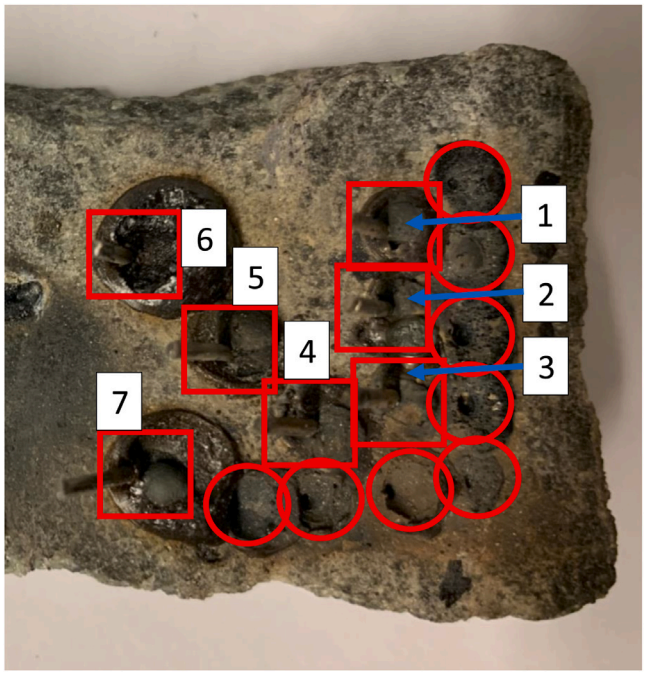

Fig. 9. The olivine sample after completion of all of the anchoring experiments. Areas marked by squares are the successful anchors and have accompanying numbers for reference. The areas marked by circles are those that did not have the strength to survive being removed from the experiment platform.

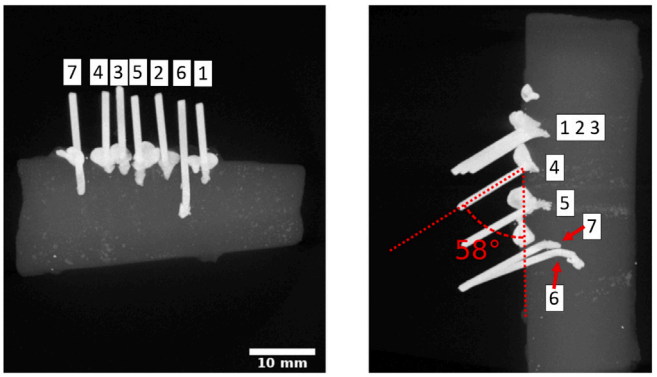

Fig. 10. XMT scans of the sample after all experiments were completed. The left image is from the right side of Fig. 9 and the right image is from the bottom side of Fig. 9.

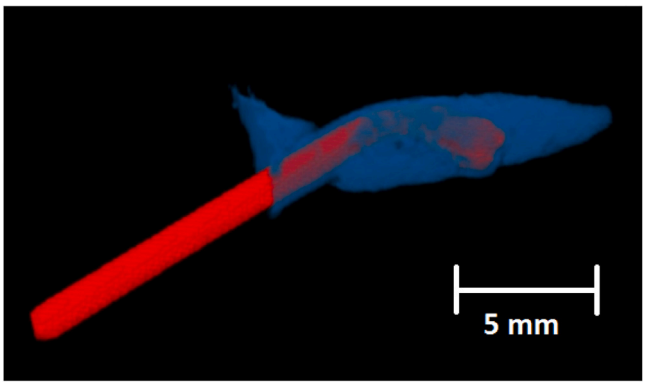

Fig. 11. XMT scan of experiment #6. The red represents the wire and the blue represents the air surrounding it.

wires near the base, which suggests it was partly melted before being pushed below the surface.

3.2.2. Anchor strength measurements

The results of the tensile testing are given in Table 3. The two methods of bending the wire tips or using an electrical conduit proved successful for all but one of the experiments: the steel plate experiment

Table 3
Results from the pullout force measurements with corresponding experiment parameters. The letters RD and F stand for "RampDown" (where the power was lowered from the power in column 2 to zero over the stated duration) and "Feed" (where the wire was fed after the laser was turned off for the stated duration).

Wire #	Power (W)	Hole time (ms)	Feed time (ms)	Post feed (ms)	Pullout force (N)
Olivine 1	1500	150	500	500 (RD+F)	85.4
Olivine 2	1500	150	500	250 (RD+F) + 250 (F)	15.0
Olivine 3	1500	150	500	500 (F)	n/a
Olivine 4	1500	250	900	500 (RD+F)	n/a
Olivine 5	1500	250	900	650 (RD+F) + 350 (RD)	83.9
Olivine 6	1500 – 4500	250	150 + 700	650 (RD+F) + 350 (RD)	115.6
Olivine 7	1500 – 3000	250	150 + 700	650 (RD+F) + 350 (RD)	113.8
Pyroxene 1	1500	250	900	250 (RD+F) + 250 (F)	7.5
Serpentine 1	1500	250	900	250 (RD+F) + 250 (F)	70.7
Steel 1	1500	250	900	250 (RD+F) + 250 (F)	>159.0

was so strong, that neither method could remain attached to the wire. The anchor strength was most likely much higher than the failed measurement result listed as lower limit. Wires #3 and #4 broke off during the attachment to the universal testing machine, and we assume their anchor strengths are <7.5 N (the lowest value recorded of all experiments).

4. Discussion

In hindsight, the wire-based moving-platform experiments would be difficult to implement in reality at an asteroid surface due to the stiffness of the wire. The wire would have to be pre-bent and "held" against the surface to match the experiment. What the high-speed imaging did reveal was that there was a lack of wetting—the molten metal would not stick to the olivine surface. Attempts to pre-heat the surface either started melting the olivine or did not help with sticking issues. Using a number of wires bundled together (more molten metal) yielded the same result. Some experiments did bind a bit of the metal to the surface as it cooled, but the holding strength was so weak that they would fall off at the slightest touch. In reality, the surface of the asteroid will not be a smooth plane, but be ragged, which could perhaps have allowed for a better bond, but the wire would not have sat flush on the surface.

The plate-based MPEs were more promising than the initial wire MPEs, but ultimately did not yield a strong anchor either. The laser spot was illuminating both the plate and the olivine below. The metal exhibited a relatively calm melt front, while the olivine was relatively chaotic. The power level used caused the olivine to sputter a significant amount of material. The olivine melt pool had vapor bubbles and cavities mixed throughout, which are not conducive to a good weld. A solidified barrier formed between the melt pools, and remained after the metal plate came off of the sample, which suggests the lip was made of olivine, and not molten metal.

The results of the feeding experiments were sensitive to the tuning of the laser and feeder parameters. For instance, it seemed necessary to keep feeding the wire after the laser was turned off, while the materials were still molten. The two experiments with the strongest bonds (wires #6 and #7 in olivine) had a feed time twice as long as the laser on time. We were unable to determine a meaningful mathematical relationship between the parameters and the resulting anchor strength, because the number of experiments was too small. It is clear that more experiments need to be performed in sufficient numbers to be able to determine an average strength for a given set of parameters.

The pyroxene experiment had a surprisingly low strength. This could be due to the fact that pyroxene can be more brittle than the other two materials, possibly due to its characteristic cleavages. Alternatively, the location could have been a natural weak point or the laser parameters were not optimized for the specific material.

We noted when handling the samples that one could wiggle the wires side to side, as if the wire did not fully fill the empty space below the surface and this was confirmed by the XMT scan shown in Fig. 11. In fact, most of the wire did not melt at all, and was simply *pushed* below the surface *after* the laser power decreased. We think that this is due to a process known in laser processing as bridging—if the hole diameter is relatively small, the surface tension of the melt pool will prevent the liquid from falling down into the hole. We attempted to address this in experiment #6 by increasing the power of the laser to induce a piercing process, where the laser would *force* the liquid down via vapor pressure. However, although the hold strength was the highest of the rock samples, there is still a lack of molten material deep in the hole as seen in the XMT scan.

We noticed that the amount of wire being fed into the system seemed greater than the calculated hole volume could handle. A considerable amount of molten metal is dissipated through various mechanisms. Some of it remains cohesive in the surface plug, some of it may mix with the molten olivine and sink into the many pores and cracks created during the laser processing.

The results of the work presented above can be compared to other anchoring techniques like those described by [3]. They report that the harpoon mechanism from the Philae lander would have been tightened up to 30 N, and that self-opposed drills have maximum strengths of up to 200 N for each drill, depending on the material drilled into. The self-opposing drills are limited by the fracture strength of the target material, which we can confirm as well in our experiments. The microspine gripper, developed at NASA's Jet Propulsion Laboratory, have hold strengths of up to 180 N depending on the surface roughness of their samples [7].

Our novel attachment mechanism demonstrated the strength of one 1.2-mm wire being pulled straight out of the hole. To create an even stronger anchor, one could consider drilling and inserting a wire diagonally, and pulling at an angle (similar to the self-opposed system described above.) Perhaps several anchors could be created in a small area, further increasing the total hold strength.

The "billowing" phenomenon seen in Fig. 8 and other experiments could be caused by a number of possible processes. It seems to occur after the laser has been shut off, and after most of the molten material has cooled and re-solidified. There could be vapor trapped beneath the surface, which is trying to escape. Perhaps it has to do with the differences in density of the melt pools (i.e., molten olivine becomes trapped below re-solidifying metal). Alternatively, it could be the solid wire being forced below the surface, pushing molten material or vapor upwards.

Future work could include studying the process on alternative target samples. Our sample selection assumes a relatively dense, monolithic asteroid or surface boulder, made mostly of silicates. In reality, we know asteroids could be porous, rubble piles, or even metallic; the anchoring efficiency on which could vary greatly. We also note that some asteroids are covered in regolith, which could be fluffy or dense, which could also be affected by a hovering spacecraft's thruster plume. It is also worth studying the effects of atmospheric pressure on the melt pool dynamics, for both sets of experiments. We used a non-volatile gas to prevent oxidation, but that does not exactly mimic the vacuous and low-gravity environment near the surface of asteroids.

5. Conclusions

1. In general, we were able to demonstrate that a laser-based wire-to-stone attachment mechanism can work.
2. Due to the lack of wetting, a surface weld or "solder" was not possible under our experimental conditions.
3. The melt pools of olivine and the tested metals would not mix under our experimental conditions. In addition, molten olivine re-solidified as a glassy material, with pores and cracks, and would thus not make a strong anchor.
4. The anchors produced in the feeding experiments had a hold strength up to 115 N when pulled along the wire axis.
5. The wire-feeding technique can be used to anchor a spacecraft to the surface of a small body, pick up or move small boulders on the surfaces of small bodies, or to redirect small monolithic asteroids or space debris.

Declaration of competing interest

The authors declare that they have no known competing financial interests or personal relationships that could have appeared to influence the work reported in this paper.

Acknowledgments

This research was partly funded by the Knut and Alice Wallenberg Foundation, and used services of the X-ray Micro-CT Laboratory at the Department of Physics, University of Helsinki.

References

[1] E. Hand, Philae probe makes bumpy touchdown on a comet, Science (ISSN: 0036-8075) 346 (6212) (2014) 900–901, http://dx.doi.org/10.1126/science.346.6212.900, eprint: https://science.sciencemag.org/content/346/6212/900.full.pdf. [Online]. Available https://science.sciencemag.org/content/346/6212/900.

[2] F. Scholten, F. Preusker, S. Elgner, K.-D. Matz, R. Jaumann, J. Biele, D. Hercik, H.-U. Auster, M. Hamm, M. Grott, C. Grimm, T.-M. Ho, A. Koncz, N. Schmitz, F. Trauthan, S. Kameda, S. Sugita, R. Honda, T. Morota, E. Tatsumi, Y. Cho, K. Yoshioka, H. Sawada, Y. Yokota, N. Sakatani, M. Hayakawa, M. Matsuoka, M. Yamada, T. Kouyama, H. Suzuki, C. Honda, K. Ogawa, The descent and bouncing path of the Hayabusa2 lander MASCOT at asteroid (162173) Ryugu, Astron. Astrophys. 632 (2019) L3, http://dx.doi.org/10.1051/0004-6361/201936757, [Online]. Available.

[3] K. Zacny, P. Chu, G. Paulsen, M. Hedlund, B. Mellerowicz, Asteroids: Anchoring and sample acquisition approaches in support of science, exploration, and in situ resource utilization, in: V. Badescu (Ed.), Asteroids: Prospective Energy and Material Resources, 2013, pp. 287–343, http://dx.doi.org/10.1007/978-3-642-39244-3_12.

[4] P. Wang, X. Chen, Q. Pan, B. Madigan, J. Long, Laser welding dissimilar materials of aluminum to steel: an overview, Int. J. Adv. Manuf. Technol. (ISSN: 1433-3015) 87 (9) (2016) 3081–3090, http://dx.doi.org/10.1007/s00170-016-8725-y, [Online]. Available.

[5] N. Anthony, J. Frostevarg, H. Suhonen, C. Wanhainen, A. Penttilä, M. Granvik, Laser processing of minerals common on asteroids, Optics & Laser Technology (ISSN: 0030-3992) 135 (2021) 106724, http://dx.doi.org/10.1016/j.optlastec.2020.106724, https://www.sciencedirect.com/science/article/pii/S0030399220313578.

[6] J. Pocorni, J. Powell, J. Frostevarg, A.F.H. Kaplan, Investigation of the piercing process in laser cutting of stainless steel, J. Laser Appl. 29 (2) (2017) 022201–1–022201–8, http://dx.doi.org/10.2351/1.4983260.

[7] A. Parness, M. Frost, N. Thatte, J.P. King, K. Witkoe, M. Nevarez, M. Garrett, H. Aghazarian, B. Kennedy, Gravity-independent rock-climbing robot and a sample acquisition tool with microspine grippers, J. Field Robotics 30 (6) (2013) 897–915, http://dx.doi.org/10.1002/rob.21476, eprint: https://onlinelibrary.wiley.com/doi/pdf/10.1002/rob.21476. [Online]. Available: https://onlinelibrary.wiley.com/doi/abs/10.1002/rob.21476.